1984

Dynamic Behavior of Labyrinth Seals in Oilfree Labyrinth-Piston Compressors

K. Graunke

J. Ronnert

Dynamic Behavior of Labyrinth Seals in Oilfree Labyrinth-Piston Compressors

Dr.-Ing. Klaus Graunke, Sulzer-Burckhardt Engineering Works Ltd, Winterthur / Switzerland

Jan Rönnert, Dipl.-Ing., Sulzer-Burckhardt Engineering Works Ltd, Winterthur / Switzerland

ABSTRACT

After a brief introduction to the basic principles of the labyrinth compressor, 3 sections are devoted to discussing various cylinder results from research into labyrinth flow and its effects on the oscillatable piston/piston rod system.

The 1st section describes theoretical studies on labyrinth flow. Computed results derived from dynamic flow processes in a cylindrical labyrinth display good coincidence with the measured results. The theoretical gas pressure and temperature histories in the labyrinth and the gas loss quantities entailed are illustrated.

Part 2 shows the radial gas forces due to labyrinth flow measured in the labyrinth. The eccentric axis-parallel piston attitude and the oblique piston attitude are compared.

The 3rd section describes the effect of gas forces on the oscillation behaviour of the piston/piston rod system. In addition to the cylindrical labyrinth, the piston also has conical zones.These generate centering forces in the gas as it flows inside the labyrinth. Two cases of the influence of these centering forces are described.

MAIN FEATURES OF OILFREE LABYRINTH PISTON COMPRESSORS

In 1935 the World's first reciprocating compressor equipped with a labyrinth piston was built. The same machine is still in operation today - compressing air in a brewery.

Over the intervening years the design of the labyrinth piston compressor has been developed and modernized. But the essential characteristics remain, now as then, the same. They are:

- oil-free compression
- no rubbing contact between piston and cylinder
- no contamination of the gas by abraded material from piston rings
- simple, robust design

How they are achieved can be seen in three main regions within the labyrinth piston machine, Fig. 1./1/*

- the motion work with the piston rod guiding system
- the barrier section between lubricated and oil-free parts
- the sealing system for reciprocating parts, such as piston rod and piston

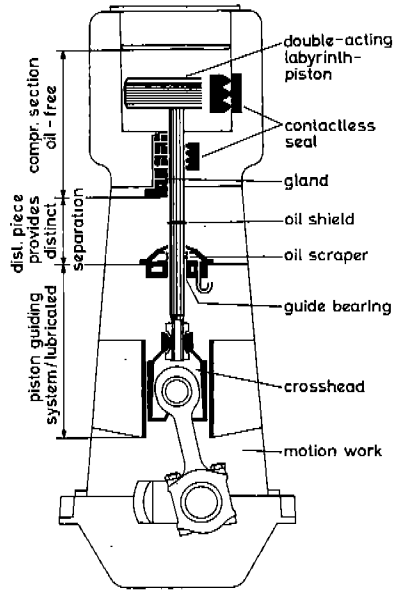

Fig. 1 Labyrinth-Piston Compressor design and constructional Features

* Numbers in brackets refer to the bibliography

The oil lubricated motion work is of unique design inasmuch as the guiding parts for piston rod and piston are concentrated exclusively in this section. By that we get the possibility that the operation inside of the compression section is free of mechanical contact between the moving parts.

Vertical motion augments the efficiency of the oil barrier system and affords completely oil-free operation of all parts in contact with the process gas. To separate the piston/cylinder group from the motion work only a simple distance piece is necessary.

He who decides to employ dry-running self-lubricating materials must accept their mechanical, thermal and chemical constraints. He is much more free to optimize the design of individual parts of his compressor when he employs the labyrinth principle with the following main features:

- avoidance of permanent mechanical friction
- ability to use materials with known, easily certifiable qualities
- wide range in piston-speed, compression temperatures and gas qualifications (chemically and physically)
- simple design of the elements exposed to the process gas.

The uncomplicated design of glands and piston is a distinguishing feature of the labyrinth piston compressor. It leads to high reliability and easy maintenance.

In the piston rod packing the key element is the labyrinth ring made of electro-graphite. According to the machine size, 3 to 6 rings are built into housing chambers. The labyrinths are cut as a fine thread on the inside of the rings.

Attached to the free end of the piston rod is the labyrinth piston. Its design is very simple, consisting normally of only three component parts, the piston skirt with the labyrinth profile, secured between two piston ends. At each end of the actual labyrinth the skirt embodies a smooth conical section. These sections form, together with the cylinder wall, converging spaces which, through the action of the compressed gas, apply a centering force to the piston.

The special construction of these machines makes it very important to know more about the interacting dynamic behaviour of the labyrinth-seals and the radial movements of piston and piston rod. It is the purpose of this paper, to tell you something about our research in this field.

PART 1. THEORETICAL DESCRIPTION OF LABYRINTH CLEARANCE FLOW

While the flow phenomena in the labyrinth have been researched in depth for steady states, no investigations into the actual dynamic conditions in the labyrinth of a reciprocating compressor have been reported to date. Besides the complicated dynamic processes in the gas, the oscillating relative motions of the two labyrinth boundary surfaces constitute a further difficulty.

For this problem an EDP computer program was to be developed, capable of calculating the pressure distribution in the labyrinth and the gas flow through it for any point in time, both for single and double-acting compressor operation. This knowledge of the gas loss rate through the labyrinth in actual compressor operation allows more accurate efficiency reflections. The pressure pattern in the labyrinth enables conclusions to be drawn about the centering or decentering effects due to the gas flowing through. A computer program of this kind permits speedy and cheap solutions to dimensioning and optimization problems.

Fundamentals

The labyrinth sealing principle can be explained with reference to Fig. 2. Owing to the small clearance, a small part of the working medium passes through the labyrinth from the high to the low-pressure side. The actual labyrinth consists of a larg number of throttling ridges on the piston, having only very little clearance with the cylinder wall, followed by a relatively big volume enlargement - the labyrinth chamber.

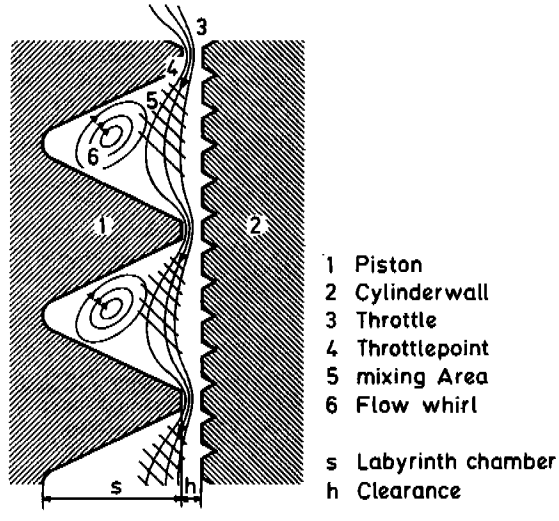

Fig. 2 Flow within the Labyrinth

The sealing action of the labyrinth may be explained as follows: due to the pressure differences from one chamber to another, the throttling point acts as a nozzle for the gas. Part of the pressure energy in the preceding chamber is converted into kinetic energy in the nozzle. In the next chamber the velocity is retarded almost to nil, and the kinetic energy is partly dissipated as heat and partly transformed to energy of a vortex. By providing a succession of these systems of throttling point and chamber, the pressure is reduced from the high level before the piston to the low level after it. More information about such throttled flows in labyrinths may be found in /2/.

This flow process in the labyrinth can be described theoretically by a few differential equations. Apart from the ideal gas equation of state, the continuity equation, the equation of motion or the momentum law, and the law of the conservation of energy have been used.

The computer program was based on the following assumptions:
- ideal gas with c_p, c_v = constant,
- heat exchange solely with the environment - no heat conduction within the gas layers,
- constant component temperatures,
- gas states outside the labyrinths are known functions of time.

Based on above assumptions, the following basic equations can be derived and programmed in a proper form.

The ideal gas equation of state yields for a constant labyrinth-chamber-volume ($dV/dt = 0$):

$$\frac{dT}{dt} = T \cdot \left(\frac{1}{p} \cdot \frac{dp}{dt} - \frac{1}{m} \cdot \frac{dm}{dt} \right) \qquad (1)$$

The energy balance and the ideal gas equation of state yield after a few transformations for the considered labyrinth chamber:

$$\frac{dp}{dt} = \frac{\varkappa - 1}{\varkappa} \cdot \frac{1}{V} \cdot \left[\frac{dm_E}{dt} h_E + \frac{dQ_K}{dt} - \frac{dQ_Z}{dt} - \frac{dm_A}{dt} h_A \right] \qquad (2)$$

According to the mathematical rules for a simple nozzle results for the mass flow of the gas:

$$\frac{dm_{E,A}}{dt} = \alpha_{E,A} \cdot w_{th_{E,A}} \cdot \varrho_{E,A} \cdot A_{E,A} \qquad (3)$$

and for the mass balance in the labyrinth chamber:

$$\frac{dm}{dt} = \frac{dm_E}{dt} - \frac{dm_A}{dt} \qquad (4)$$

The flow of heat from the labyrinth piston- and the cylinder wall-surface resp. to the gas can be computed as follows:

$$\frac{dQ}{dt} = \alpha_w \cdot A_w \cdot \left(T_w - T_G \right) \qquad (5)$$

For the gas velocity in the nozzle applies the following slope function:

$$w_{th} = f\left(x, p, \frac{dx}{dt} \right) \qquad (6)$$

Because smooth, tapered piston elements are employed in the labyrinth piston compressor to ensure better guiding, the pressure pattern and loss coefficient mustbe calculated for these parts of the piston too. These formulations were also integrated in the computer program.

Calculation Results

In Fig. 3 the measured and calculated leakage rates through a labyrinth steady flow are compared. The leakage losses are plotted versus different labyrinth lengths. The measured results are of older date (/3/ Fig. 26).

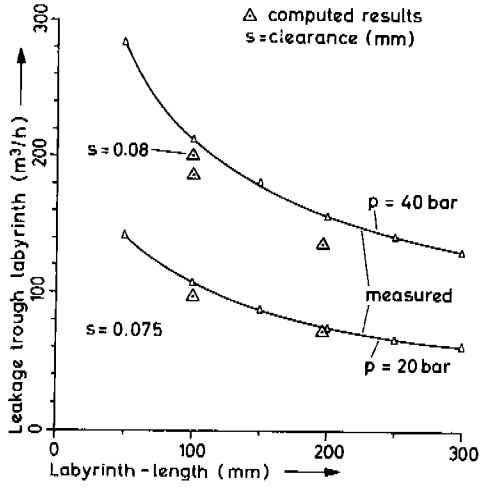

Fig. 3 Leakage at different Pressure in Funktion of Labyrinth-Length

Here over all pressure difference and profile form were varied as parameters. Comparative calculations were performed for one profile. Though the results show good agreement with the measurements, a calculation with a labyrinth clearance 0.005 mm bigger yielded even closer agreement. Here the measuring tolerancerance when determining the labyrinth clearance might be pointed out.

The clearance may also be increased by possible dilation of the cylinder by the high pressure, so that the calculated values lie within the tolerance range of the previous measurements.

For the dynamic investigations a comparison must be made likewise between calculation and measurement. Accordingly, a measured dynamic pressure curve in the labyrinth of a single-acting compressor stage is plotted in Fig. 4.

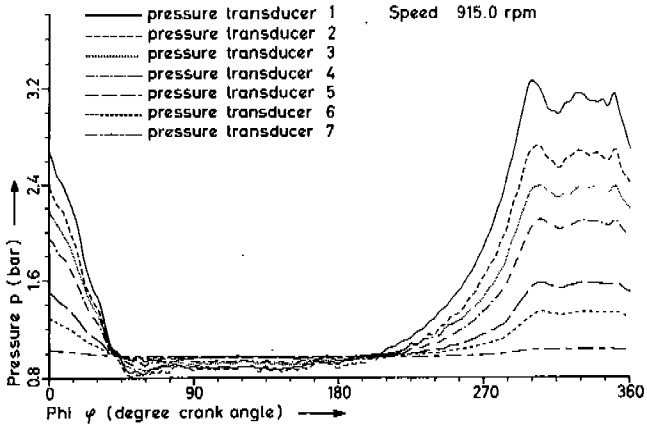

Fig. 4 Measured Dynamic Pressure for one Revolution in the Testlabyrinth

A labyrinth with 50 chambers was examined. Pressure transducer 1 gives the pressure behaviour in the compression chamber before the labyrinth, while transducers 2 to 7 detected the pressure in the 13th, 23rd, 33rd, 43rd, 46th and 49th labyrinth chambers. The calculation performed for the same boundary parameters yields a result according to Fig. 5.

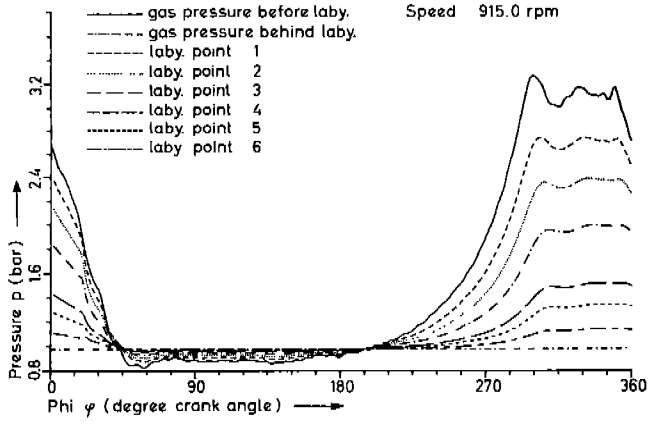

Fig. 5 Computed Dynamic Pressure for one Revolution in the Testlabyrinth

The pressure curves were plotted for the same chambers as investigated with the measurements (designated "laby. point"). Here the results from pressure transducer 1 in Fig. 4 are input of the calculation. The agreement is good. Only in the last third of the labyrinth length are differences observable during higher pressure differences on the test piston (laby. point 4 and 5). In Fig. 6 the corresponding calculated temperature curve in the labyrinth is shown.

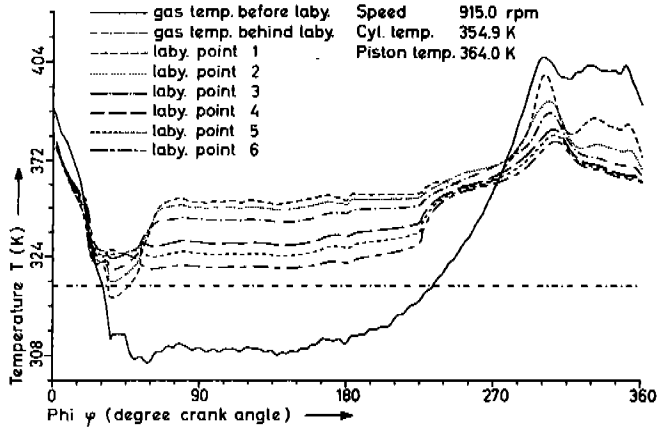

Fig. 6 Computed Dynamic Temperature for one Revolution in the Testlabyrinth

Here the influence of the cylinder and piston surface temperatures on the gas temperature in the labyrinth is very clear. From about 60° to 200° crank angle (compressor intake phase) gas flows from the leakage collector with constant gas condition to the labyrinth, and through this back into the compression volume of the compressor. During this it is heated by the high wall temperatures. Equally during the compression phase of the compressor the gas is cooled in the labyrinth. The effect of a temperature reduction due to throttling is negligible here. On the whole, calculations with variation of the component temperatures show that the dynamic temperature curves vary only within narrow limits.

With the computer program described here it is possible for the first time to investigate theoretically the dynamic flow phenomena in the labyrinth of a labyrinth-piston compressor. Besides the gas states outside the labyrinth varying in time, the piston motion is taken into account also. Comparison of the calculated results with measurements shows satisfactory agreement.

Parameter studies may now be carried out. Consequently the effects of all kinds of compressor variables on the labyrinth gas leakage rate and the pressure patterns within the labyrinth during dynamic operation can be determinded.

PART 2: MEASUREMENT IN A LABYRINTH WITH CYLINDRICAL PISTON

As the theoretical investigation of the labyrinth leakage flow the experimental investigation of the dynamic behaviour of the labyrinth leakage flow is likewise aimed at researching the labyrinth geometry with regard to sealing efficiency and radial gas forces. Further the test results are used to examine the accuracy of the theoretical investigation.

For this it is necessary to establish the pressure distribution in the labyrinth in the axial and circumferential directions. This must be performed as a function of the crankshaft angle and of the moving piston standing eccentrically in the cylinder bore. From the pressure distribution on the piston skirt a radial gas force results finally, responsible for the centering and decentering effects of the medium on the labyrinth piston.

Measuring Rig

For the experimental investigation of the labyrinth leakage flow a rig had to be developed enabling to measure the pressure pattern in the labyrinth in the axial and circumferential directions of the piston (the radial gas force on the piston resulting from it) and the labyrinth leakage rate for any position of the piston in the cylinder bore.

It must be possible to expose the labyrinth to static and dynamic pressure sequences. Measurements directly on the acting compressor piston are not reproducible and therefore without point. Another difficulty was experimental detection of the radial gas forces, which are very small compared with the axial gas forces. A further requirement is the use of pressure transducers capable of measuring both static and dynamic pressures with adequate accuracy These sensors must be sufficiently small to allow measuring the pressure in one chamber only without difficulty.

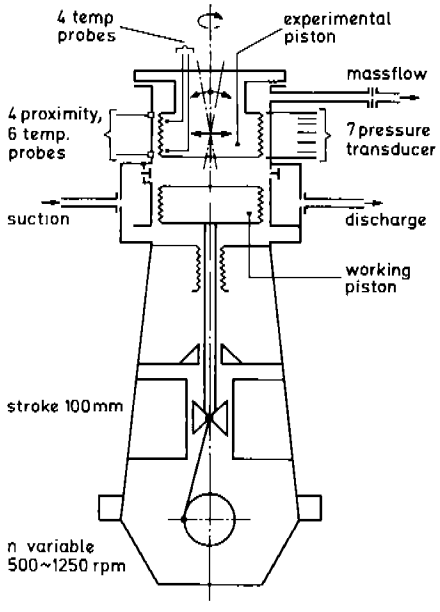

Fig. 7 Cross-Sequential Diagram of Test-Equipment

In view of these demands a measuring rig was designed for fitting on the cylinder of a 1D100-1A compressor in place of the cover. The compressor serves merely to generate the dynamic pressure behaviour. With this conception the measurement of the axial piston motion is ignored (Fig. 7).

The radial gas forces on the piston are not measured directly but calculated from the pressure patterns in the axial and circumferential directions. To keep the amount of measuring elements within limits only one measuring plane was fitted with pressure transducers and the different clearances at the piston circumference were brought successively to this plane. One of these sensors detects the pressure before the test labyrinth. Six others are distributed purposefully over the length of the labyrinth.

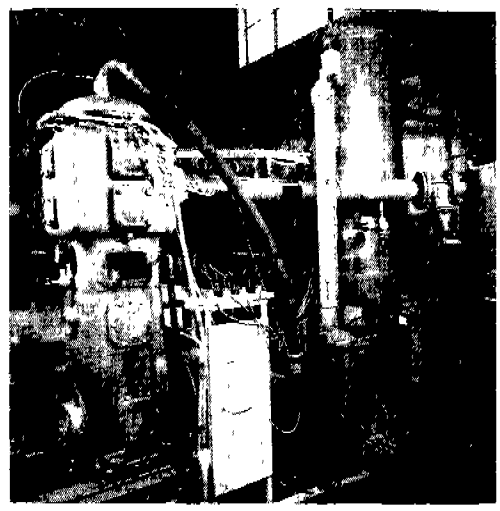

Fig. 8 Total View of the Test-Bench

Fig. 8 gives a general view of the test stand, looking at the intake side of the compressor where the measuring plane of the test rig is located. The tube to the measuring device for the labyrinth leakage rate is easily recognizable.

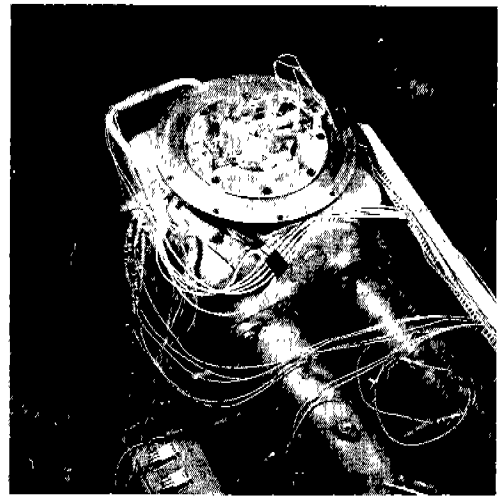

Fig. 9 Measurement Device for the Labyrinth-Flows

In Fig. 9 the cover of the test rig has been removed. Four thermocouples for detecting the piston temperatures are seen.

In the test cylinder an annular disk is mounted rotatably, with the upper piston crown fixed on it. The latter is cross-shaped, as shown here, and the cross may be moved radially, enabling eccentric piston positions to be adjusted. By turning the annular disk the different clearances on the piston circumference are then brought to the measuring plane.

Two pairs of displacement sensors are fitted in the test cylinder in two planes at 90° to each other, so that the exact position of the test piston in the bore can be determined at any time. One pair of displacement sensors is monted in the pressure measuring plane.

The labyrinth consists of 50 chambers spaced at 2,0 mm, resulting in an overall labyrinth length of 100 mm. The pressure transducers detect the pressure behaviours in the 13th, 23rd, 33rd, 43rd, 46th and 49th chamber, counting from the compression side.

Dynamic Measurements

Fig. 4 shows the pressure measured in the labyrinth plotted against the compressor crankshaft angle (ca). One revolution is graphed, with top dead centre at $\varphi = 0^{\circ}$ ca. Transducer 1 gives the pressure behaviour before the labyrinth, i.e. in the cylinder of the compressor. Transducers 2 to 7 measure the pressures in the labyrinth.

At other test series the eccentricity, revs per minute and pressure difference at the test labyrinth are varied, measuring the pressure in the labyrinth at different circumference angles each time.

When the diagrams for $p = f(\varphi)$ are examined it will be noticed that the storage effect of the labyrinth chambers and hence the dead time effect are only very small. This can be recognized only through the different intervals between the curves during reexpansion compared with compression. Evaluation of the measurements gives a time lag of 0.008 ms per labyrinth chamber or $\varphi = 0.04^{\circ}$ crankshaft angle per chamber. This means the behaviour of the pressure in the labyrinth against the time scale is very similar to that in the cylinder.

From these curves for fixed times (crank angles) the pressure patterns in the labyrinth can now be determined in the axial direction at the different piston circumference angles. The pressure distribution at the piston circumference within the labyrinth obtained in this way enables the resulting radial gas force on the piston to be calculated.

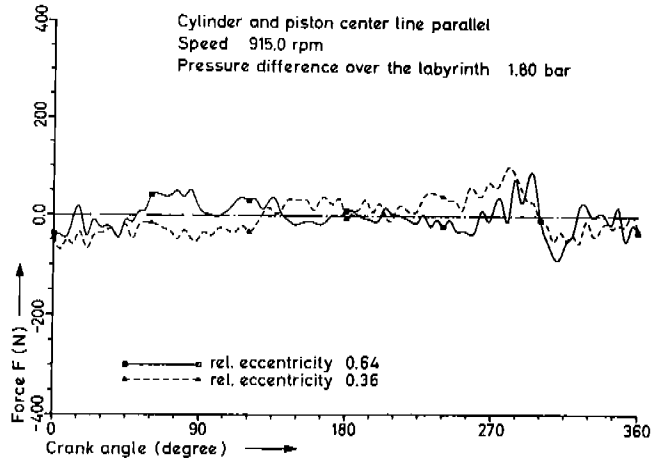

Fig. 10 Radial Aerodynamic Force in Function of Crank Angle on Labyrinth-piston

This radial gas force can be determined for any crank angle. Fig. 10 plots the force vs. crank angle during one revolution, for two eccentric piston positions with cylinder and piston axes parallel. It will be seen from this diagram that the force varies around nil with small scatter. No correlation is apparent with the pressure vs. time behaviour (Fig. 4) in the labyrinth. Altering the eccentric piston position has no effect either. It is therefore clear that only a negligible radial gas force is present with axis-parallel eccentric piston attitude.

As with the previous steady-state measurements not shown here, in the dynamic tests too there is a perceptible difference in the pressure distribution at the piston circumference when the piston. is canted a little (0.08°). In this case, however, the pressure difference at the labyrinth plays a big part. The differences in the axial pressure pattern at the piston circumference grow in proportion to the pressure difference, with the curve in the divergent clearance flatter than in the converging gap.

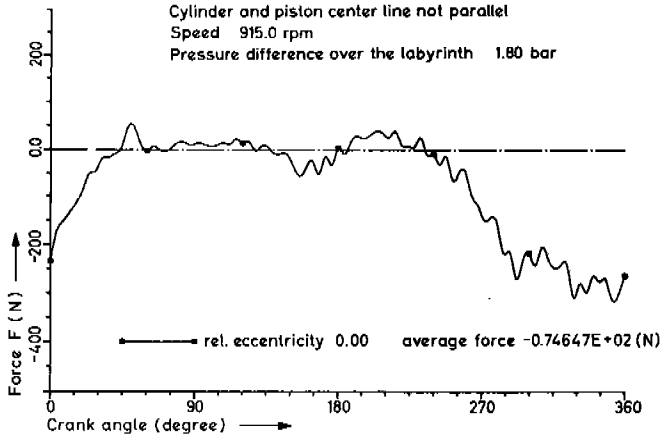

Fig. 11 Radial Aerodynamic Force in Function of Crank Angle on Labyrinth Piston

The dynamic radial force pattern during one revolution (Fig. 11) differs very much from that of the axis-parallel piston attitude (Fig. 10). Whenever there are substantial pressure differences on the labyrinth, major radial gas forces are sustained by the piston. Only during the compressor intake phase are they around nil.

As may be seen, the radial resulting force on the piston follows the pressure pulsation in the labyrinth pretty exactly, so that there is a pulsed force excitation.

As this excitation always takes place in the direction from the converging to the diverging clearance, it is probable that the piston will touch the cylinder wall.

It is possible, to prevent the tendency of canting of the piston in the cylinder with a series of proven provisions.

Labyrinth Leakage Rates

The measured labyrinth leakage rates are presented as mean values. Thus Fig. 12 plots the labyrinth leakage vs. relative piston eccentricity in the cylinder.

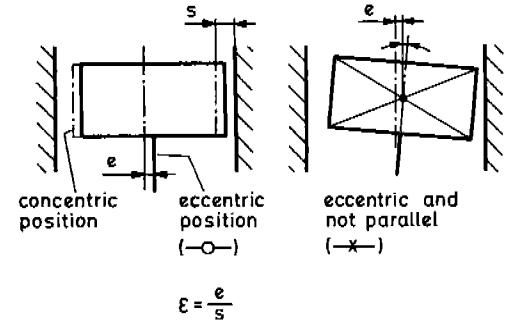

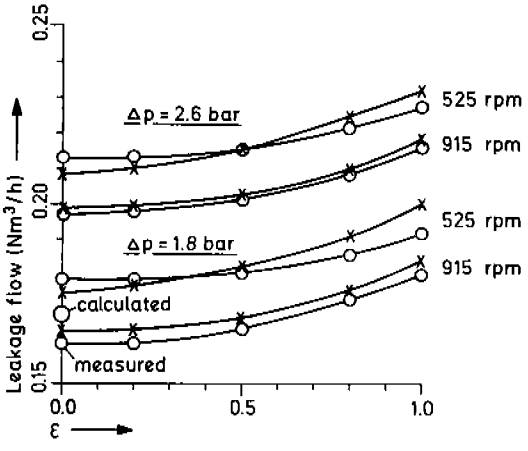

Fig. 12 Leakage Flow through Labyrinth in Function of the relative Eccentricity.

The measured leakage show a tendency to increase with growing eccentricity, though the increase is relatively small. Logically, the flow rate is higher with a large pressure difference than with a small one. With canted piston the flow rate rises slightly more with growing eccentricity than with axis-parallel piston.

To sum up it can be said that the labyrinth leakage correlates proportionally to the clearance subproportionally with revs per minute and pressure difference and weakly progressive with the eccentricity. The clearance and with it all parts which vary the clearance during operation are the dominating parameters for the labyrinth leakage rate.

PART 3: OSCILLATIONS IN THE PISTON/PISTON ROD SYSTEM

The piston rod, guided at its lower end by the crosshead and beneath the cylinder by a slip bearing (Fig. 1 and 13) forms in conjunction with the piston attached as an overhung mass to its upper end, a flexurally elastic, oscillatable system. For the perfect operation of the compressor the piston should be kept free of contact with the cylinder.

As the piston moves, its distance from the piston rod bearing alters periodically. In other words, the flexural elasticity of the piston rod modifies with the reciprocating motion of the piston. If the piston is positioned slightly askew, the pressure pulsations of the propellant gas in the cylinder may give rise to radial forces on the piston, exciting the system to oscillate. Because the flexural elasticity of the piston rod is not constant, the oscillations may become unstable.

The flexural oscillations of the system due to excitation by the vibrations of the machine casing were the subject of an earlier analytical study /4/.

Here a study is made of the excitation forces acting directly on the piston. Calculation of the chronological evolution of piston motion under the influence of a pulsating radial force is discussed.

Motion Equation

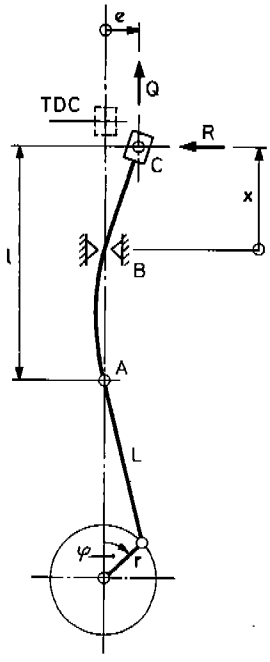

Fig. 13 Motion Work Scheme

Fig. 13 shows a diagram of the motion work, where A is the crosshead and B the piston rod guide bearing underneath the cylinder. Guidance of the piston rod AC in the bearings A and B is assumed to be articulated and backlash-free. The distance x between the piston C and the bearing B is a function of the rotation angle φ of the crankshaft r and therefore varies as a function of time t.

Q and R are the excitatory vibration forces acting on the piston.

Axial Force

The axial force Q consists of the differential gas force acting on the piston head and the inertial force of the piston. Its influence on the flexure of the piston rod is in comparison with the radial forces relatively small and will be, for simplicity, neglected here.

Radial Force

Mention has already been made of the fact that if the piston is positioned slightly askew, a pulsating radial force proportional to the pressure differential at the piston can be generated.

Under its influence the piston is forced out of its central position. As a result of this radial movement an internal radial elastic force, the product of piston rod flexure and a radial piston inertial force, is generated.

In accordance with Newton's Law of Motion the following motion equation for a piston mass m_r is obtained.

$$m_r \frac{d^2e}{dt^2} + D \frac{de}{dt} + e \frac{3EJ}{lx^2} = f(\Delta p) \qquad (7)$$

The right-hand side of equation (7) shows the excitation gas force as a linear function of the differential pressure Δp at the piston. A term proportional to transverse piston velocity has been inserted for damping.

(7) is a non-homogeneous differential equation of the second order with one perturbation component.

Numerical Solution of the Motion Equation

To determine the chronological evolution of piston deflection e from its central position, a computer program was developed to solve the motion equation numerically and plot the track of the piston as a function of time and of piston travel, respectively. Instead of taking e as an absolute eccentricity figure, relative eccentricity

$$\varepsilon = \frac{e}{R - r} \qquad (8)$$

was inserted into the equation to be solved. R - r is the radial play of the piston in the cylinder.

The calculation was carried out for an example consisting of a vertical, single-acting compressor.

In the left-hand portion of Fig. 14 the evolution of the excitation gas force in relation to stroke is shown as a line of dashes. In the right-hand portion of Fig. 14 the line of dashes represents the evolution of relative eccentricity,

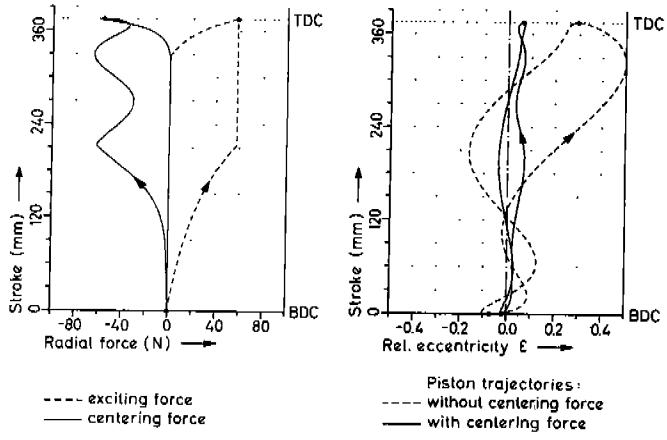

Fig. 14 Piston Paths and the Exciting and Centering

Centering Effect of the Smooth Cones

It was determined experimentally and confirmed theoretically that smooth conical sections at the ends of the piston shell exert a centering effect. The centering force emerged as a function of the relative eccentricity ε and the pressure differential at the piston, as follows.

$$Z = \varepsilon \cdot \left(a \cdot \Delta p^2 + b \cdot \Delta p\right) \qquad (9)$$

a and b depend on the geometry of the relevant machine.

Reference is again made to Fig. 14. The continuous curve on the right-hand side shows the path of the piston allowing for the centering action of the cones. The continuous curve on the left-hand side shows the evolution of the centering forces at the cones. It is observable that the centering force rises as eccentricity increases.

In consequence, the centering effect of the cones makes an important contribution to ensuring that the piston moves without touching the cylinder wall.

Initial Eccentricity

Shown hereunder are the results of a calculation in which the centering effect of the smooth cones can be clearly observed (Fig. 15). An initial static eccentricity of a single acting compressor was investigated.

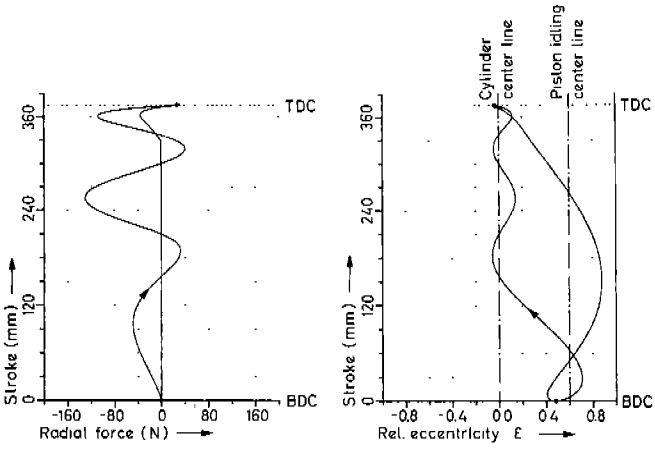

Fig. 15 Exciting Force and Piston Path Resulting from an Initial Eccentricity

The right-hand side portion of Fig. 15 shows the stabilized piston path. On the left-hand side the evolution of the centering force is to be seen. The arrows show the direction of movement. At the BDC the pressure differential at the piston approximates to zero. Correspondingly, the centering force starts at zero and rises in accordance with the increasing pressure in the cylinder. During this phase the piston is pushed towards the axis of the cylinder.

As soon as the center point of the piston crosses the cylinder axis, the direction of the centering force changes correspondingly. During the further progress of the power stroke the piston is held near the cylinder axis. In the right-hand portion of Fig. 15 the light oscillations of the piston round the cylinder axis are visible. On the left the related oscillations of the centering force can be recognized. Whenever the piston path crosses the cylinder center line, the sign of the centering force changes. Immediately after the TDC has been exceeded, the tendency of the pressurized gas to hold the piston in its central position is still recognizable. Later on during the intake phase the pressure differential at the piston is nearly zero. Hence the centering force diminishes also to zero and the piston swings back to its initial position without resistance.

The extremely large value of the initial static eccentricity (0,6) can in reality never occur. It has been chosen on purpose just to prove, that even on this extreme condition the piston would not touch the cylinder walls.

Final Observations

It has been demonstrated that the dynamic behaviour of a labyrinth compressor piston/piston rod system can be elucidated theoretically. Using suitable features in the design of the piston it is possible to achieve a self centering effect which helps to keep the piston free of contact with the cylinder. The results represent a small selection derived from the studies currently in progress. Extensions to the computing program embody allowances for the lubricating oil film at the crosshead and guide bearing and for the influence of the axial forces in the system. Computed results embodying all these parameters plus measured results for comparison purposes will be reported at a later date.

NOTATION

A Cross-sectional area of the throttle
A Surface area of piston or cylinder in considered labyrinth chamber
a Coefficient
b Coefficient
D Coefficient of damping
E Modulus of elasticity
e Piston eccentricity
h Specific enthalpy
J Moment of inertia
l Length of piston rod
m Mass
p Pressure
Q Heat
R Radius of cylinder bore
r Radius of piston
t Time
T Temperature
V Volume
w Velocity
x Distance of piston from TDC
Z Centering force
α Flow coefficient
α_W Coefficient of heat convection
ε Relative eccentricity
$\varkappa$ Ratio of specific heats
ϱ Density

Indices

E Inlet
A Outlet
K Piston
Z Cylinder
W Wall
G Gas
r Reduced
th Theoretical

REFERENCES

/1/ Ernst, P.: Special gas Compression Problems Solved with Oilfree Labyrinth Piston Compressors I Mech. E Conference Publication 1984-2 Second European Congress on Fluid Machinery for the Oil, Petrochemical and Related Industries 26.-28.3.84, The Hague, Netherlands

/2/ Trutnovsky, K.; K. Komotori: Berührungsfreie Dichtungen (Contactless Sealing) VDI-Verlag, Düsseldorf, 4. Auflage 1981

/3/ Walti, F.O.: Der ölfreie Kolbenkompressor (The Oilfree Piston Compressor) Schweizerische Bauzeitung 70 (1952) 16, p. 222-226

/4/ Chen, Y.,N.: Schwingungen im System Kolben-Kolbenstange ölfreier Kompressoren (Oscillations in the Piston/Piston Rod System of Oilfree Compressors) Technische Rundschau Sulzer 40 (1958) 2